RadioGraphics

US of the Elbow: Indications, Technique, Normal Anatomy, and Pathologic Conditions[1]

Gabrielle P. Konin, MD • Levon N. Nazarian, MD • Daniel M. Walz, MD

ONLINE-ONLY SA-CME

See www.rsna.org/education/search/RG

LEARNING OBJECTIVES

After completing this journal-based SA-CME activity, participants will be able to:

- Describe the normal US anatomy of the elbow.
- Discuss the US technique for evaluation of the elbow.
- Recognize the US appearances of various pathologic conditions about the elbow and their possible US-guided interventions.

TEACHING POINTS

See last page

The elbow, a synovial hinge joint, is a common site of disease. Ultrasonography (US) has become an important imaging modality for evaluating pathologic conditions of the elbow. This powerful imaging tool has the advantages of outstanding spatial resolution, clinical correlation with direct patient interaction, dynamic assessment of disease, and the ability to guide interventions. Unlike most other imaging modalities, US allows the contralateral elbow to be imaged simultaneously, providing an internal control and comparison with normal anatomy. A useful approach to US evaluation of the elbow is to divide it into four compartments: anterior, lateral, medial, and posterior. US of the elbow has varied clinical applications, including evaluation and treatment of lateral and medial epicondylitis, imaging of biceps and triceps musculotendinous injuries, evaluation of ulnar collateral ligament laxity, diagnosis of joint effusions and intraarticular bodies, and evaluation of peripheral nerves for neuropathy and subluxation. US can also be used to evaluate soft-tissue masses about the elbow. Knowledge of the normal US anatomy of the elbow, familiarity with the technique of elbow US, and awareness of the US appearances of common pathologic conditions of the elbow along with their potential treatment options will optimize radiologists' diagnostic assessment and improve patient care. Supplemental material available at *http://radiographics.rsna.org/lookup/suppl/doi:10.1148/rg.334125059/-/DC1*.

Abbreviations: DBT = distal biceps tendon, LUCL = lateral ulnar collateral ligament, PIN = posterior interosseous nerve, RCL = radial collateral ligament, UCL = ulnar (medial) collateral ligament

RadioGraphics 2013; 33:E125–E147 • **Published online** 10.1148/rg.334125059 • **Content Codes:** MK US

[1]From the Department of Radiology, Thomas Jefferson University Hospital, Philadelphia, Pa (G.P.K., L.N.N.); and Department of Radiology, North Shore University Hospital, Manhasset, NY (D.M.W.). Recipient of a Certificate of Merit award for an education exhibit at the 2009 RSNA Annual Meeting. Received April 10, 2012; revision requested May 10; final revision received January 2, 2013; accepted January 28. For this journal-based SA-CME activity, the authors, editor, and reviewers have no financial relationships to disclose. **Address correspondence to** G.P.K., Hospital for Special Surgery, 535 E 70th St, New York, NY 10021 (e-mail: *koning@hss.edu*).

Introduction

Ultrasonography (US) is an excellent imaging modality for evaluation of elbow joint and soft-tissue disease. Use of high-frequency linear transducers along with the superficial location of the elbow results in outstanding image resolution. US is advantageous in time, cost-effectiveness, accessibility, and patient comfort and can be an alternative for patients who are claustrophobic or have contraindications to magnetic resonance (MR) imaging. Direct patient interaction allows direct correlation with the site of pain, comparison with the contralateral elbow, guided interventions, and dynamic real-time assessment. Dynamic US imaging allows use of stress maneuvers and visualization of transient conditions that may not otherwise be revealed during static examination. Although operator dependence and a steep learning curve can limit use of US, the advantages are such that it continues to be increasingly used as an alternative or adjunct to MR imaging.

US allows ready evaluation of the three elbow articulations (radiocapitellar, ulnotrochlear, and proximal radioulnar) and their capsular investment for joint effusions, synovitis, and intraarticular bodies. US may be used for detection of ligamentous, muscle, and tendon disease, including epicondylitis and distal biceps and triceps musculotendinous tears. Nerves can be assessed for entrapment and subluxation with dynamic real-time US. Evaluation of osseous abnormalities—particularly in the pediatric population—is also possible with US, although it is somewhat limited in comparison with evaluation with other imaging modalities.

In this article, we present the US examination technique, normal US anatomy, and imaging findings and treatment of common diseases affecting the elbow. Specific topics discussed are US technique; anatomy of the anterior, lateral, medial, and posterior elbow; tendon and muscle disease; ligamentous disease; joint and bursa disease; peripheral nerve disease; and miscellaneous conditions.

US Technique

US examination of the elbow joint may be performed with the patient seated and the elbow placed on an examination table or with the patient supine. A high-frequency linear transducer of 12–17 MHz is ideal. Various US techniques such as extended field of view, spatial compound sonography, and harmonics may enhance diagnostic imaging (1). For the most superficial structures, a compact linear ("hockey stick") probe or large amounts of gel are useful.

Owing to the curvilinear contours of the elbow, tendons and ligaments are predisposed to anisotropy and careful scanning technique is critical. These angle-dependent structures demonstrate characteristic hyperechoic fibrillar echotexture when imaged perpendicular to the ultrasound beam, since the beam is maximally reflected. However, as the incident angle veers away from 90°, anisotropy occurs, with tendons and ligaments appearing iso- or hypoechoic to muscle (1). To avoid this common pitfall, the transducer can be gently rocked along the long axis of the tendon or ligament in question; if the hypoechogenicity persists, an abnormality is diagnosed.

Imaging the contralateral elbow can often be useful to compare the pathologic elbow with the asymptomatic normal one. Dynamic imaging is particularly helpful in assessing the collateral ligaments, subluxation of the ulnar nerve or triceps tendon, and intraarticular bodies.

US of the elbow is generally tailored to the clinical question or area of symptoms. However, a complete evaluation of the elbow should always be considered, in which case a useful approach is to divide the elbow systematically into anterior, lateral, medial, and posterior compartments (Table). The anatomy of each compartment is reviewed, followed by discussion of common pathologic conditions.

Anterior Elbow

The key structures to be evaluated anteriorly include the anterior joint recess, distal brachialis muscle, distal biceps brachii muscle, and median nerve (Fig 1). To begin US examination of the anterior elbow, the elbow is extended and the forearm is supinated (Fig 2). The examination should include both transverse and longitudinal planes extending at least 5 cm proximal and 5 cm distal to the joint (2).

To assess the radiocapitellar joint laterally and ulnotrochlear joint medially, scanning is best

Important Structures and Common Pathologic Conditions of the Elbow by Compartment

Compartment	Important Structures	Common Pathologic Conditions
Anterior	Distal biceps muscle and tendon	Tear of the DBT
	Brachialis muscle	Bicipitoradial bursitis
	Median nerve	Median nerve entrapment
	Anterior joint recess	
Lateral	Common extensor tendon	Lateral epicondylitis
	Lateral collateral ligamentous complex	LUCL tear
	Radial head and annular recess	RCL tear
	Capitellum	Osteochondritis dissecans
	Radial nerve and PIN	Radial nerve or PIN entrapment
Medial	Common flexor tendon	Medial epicondylitis
	Anterior band of the UCL	UCL injury
Posterior	Distal triceps tendon	Distal triceps tendon tear
	Posterior joint recess	Joint effusion with or without intraarticular bodies
	Olecranon bursa	Olecranon bursitis
	Ulnar nerve	Ulnar nerve dislocation

Note.—DBT = distal biceps tendon, LUCL = lateral ulnar collateral ligament, PIN = posterior interosseous nerve (deep motor branch of the radial nerve), RCL = radial collateral ligament, UCL = ulnar (medial) collateral ligament.

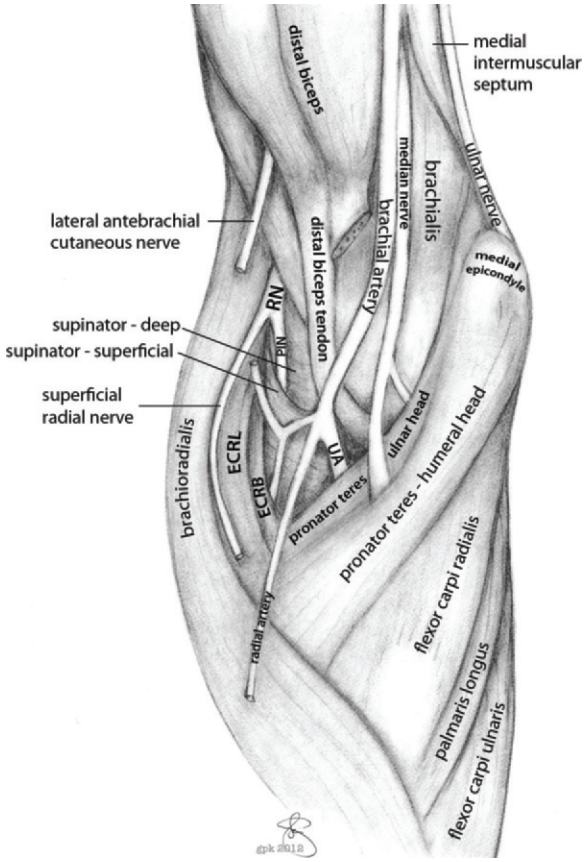

Figure 1. Deep structures of the anterior elbow. *ECRB* = extensor carpi radialis brevis, *ECRL* = extensor carpi radialis longus, *RN* = radial nerve, *UA* = ulnar artery.

Figure 2. Transducer technique for US of the anterior structures of the elbow in the long axis.

performed in the longitudinal axis (Fig 3). A thin layer of hypoechoic hyaline cartilage covers the hyperechoic subchondral bone plate of the articular surface. Overlying the hypoechoic cartilage is a thin hyperechoic line representing the anterior joint capsule, which averages 2 mm in thickness in the adult population (3).

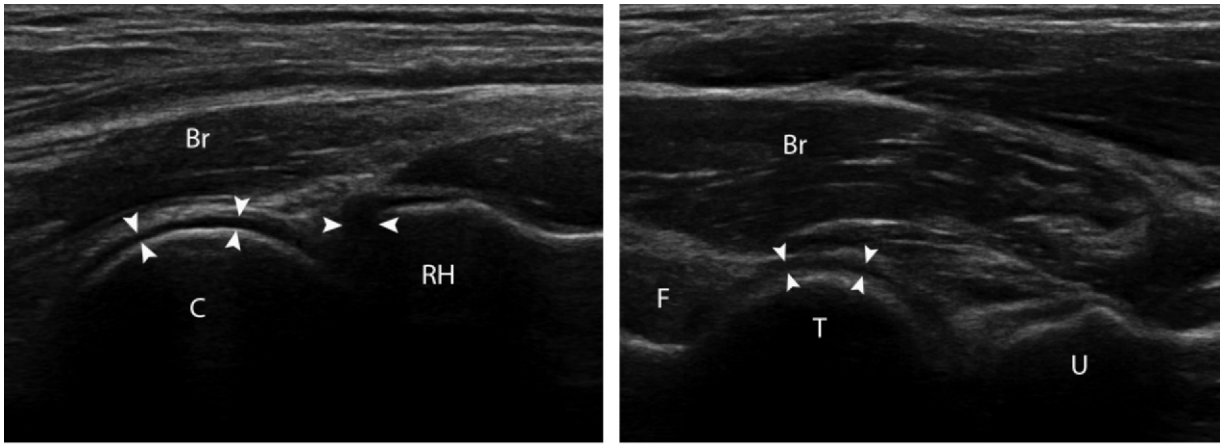

a. b.

Figure 3. Normal radiocapitellar and ulnotrochlear joints. **(a)** On a longitudinal US image of the radiocapitellar joint, the hyaline cartilage (arrowheads) appears as a thin hypoechoic band superficial to the hyperechoic cortex and deep to the hyperechoic joint capsule. *Br* = brachialis muscle, *C* = capitellum, *RH* = radial head. **(b)** Longitudinal US image of the ulnotrochlear joint shows a hyperechoic anterior fat pad *(F)* within the coronoid fossa. The characteristic appearance of muscle tissue is seen in the brachialis muscle *(Br)*. *T* = trochlea, *U* = ulna, arrowheads = hyaline cartilage.

Within the anterior joint recess, the coronoid fossa and smaller radial fossa are seen as concavities in the distal humerus. Intracapsular extrasynovial elbow fat pads are found between the hypoechoic synovial lining and hyperechoic linear fibrous capsule within the fossae. They are hyperechoic and triangular and are displaced with distention of the joint (4,5). A small amount of normal fluid may be seen between the anterior fat pad and humerus (2).

The bursae found in the cubital fossa include the bicipitoradial bursa and the less significant interosseous bursae. The bicipitoradial bursa is located between the DBT and anterior radial tuberosity and functions to reduce friction during pronation and supination of the forearm (6). Normal elbow bursae are not routinely visualized at US.

The brachialis muscle, which primarily functions to flex the elbow joint, is best evaluated with the transducer in the longitudinal plane over the anterior supracondylar region of the distal arm. The brachialis muscle lies deep to the biceps brachii and anterior to the humerus. Both the brachialis and biceps brachii muscles and tendons are located between the brachioradialis laterally and pronator teres medially. The brachialis is the larger of the two muscles, both of which demonstrate hypoechoic muscle fascicles with intervening hyperechoic fibroadipose septa, findings characteristic of muscle tissue. The brachialis can be imaged in the transverse and longitudinal planes to its insertion on the proximal ulna (Figs 3, 4).

The DBT primarily acts to flex the elbow but also to supinate it. It is best evaluated with the patient's forearm in maximal supination to bring the tendon insertion at the radial tuberosity into view. The biceps muscle is located superficial to the brachialis muscle and lateral to the brachial artery and median nerve (Figs 4b, 5). The DBT is formed by union of two muscle bellies: the short and long heads of the biceps brachii. Persistent division of the short and long heads of the DBT is an important anatomic variant to be aware of to avoid incorrect diagnosis as a DBT partial tear (7).

The DBT is covered by an extrasynovial paratenon and is approximately 7 cm long, fanning out at its insertion on the radial tuberosity over an area of 3 cm^2 (8). At the myotendinous junction of the DBT, there is a flattened aponeurotic expansion, the lacertus fibrosus, which extends to the medial deep fascia of the forearm. It covers the median nerve and brachial artery and plays an important role in maintaining the DBT in its appropriate position (1).

US of the distal DBT can be technically challenging due to its steep oblique course and 90° rotation (9). It is best evaluated in the transverse plane. Without meticulous scanning technique, particularly in the sagittal plane, anisotropy may result in misdiagnosis as a tear or tendinosis. To avoid this pitfall, the transducer should be posi-

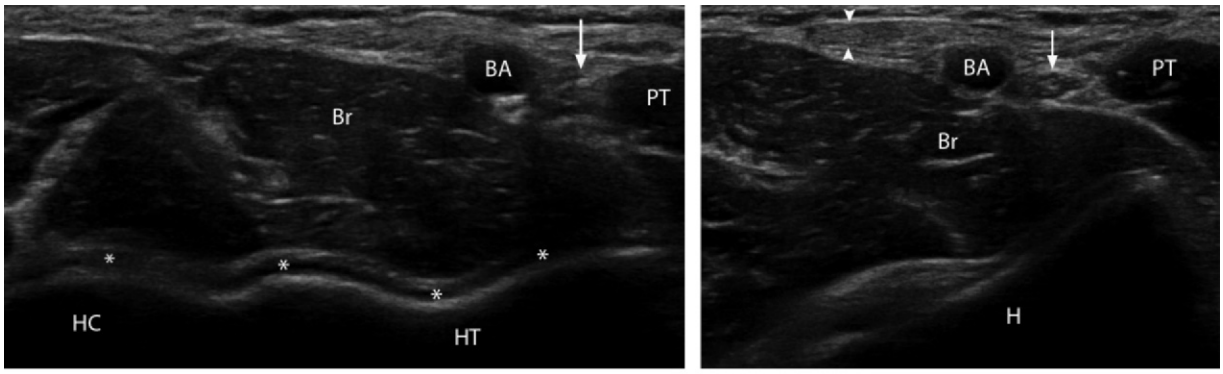

a. b.

Figure 4. Normal structures of the anterior elbow. **(a)** Short-axis (transverse) US image shows the distal humerus, which appears as a wavy hyperechoic line covered by thin hypoechoic articular cartilage (∗). Note the rounded surface of the lateral humeral capitellum *(HC)* and the V-shaped humeral trochlea *(HT)*. The brachialis muscle *(Br)* has the typical appearance of muscle tissue in the short axis. The median nerve (arrow) is medial to the brachial artery *(BA)* and has a fascicular appearance. *PT* = pronator teres. **(b)** Short-axis US image shows the hyperechoic DBT (arrowheads) lateral to both the brachialis artery *(BA)* and median nerve (arrow). Note the characteristic speckled fascicular appearance of the median nerve. Deep to the DBT is the brachialis muscle *(Br)* with its characteristic hypoechoic appearance and intervening fibrofatty septa. *H* = humerus, *PT* = pronator teres.

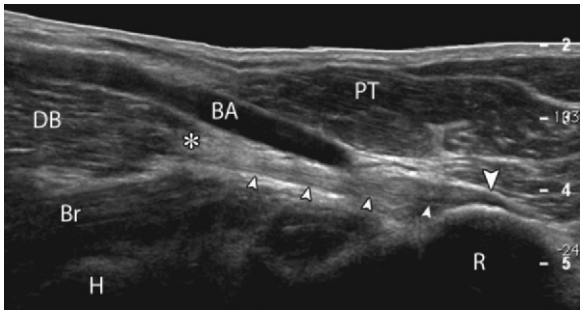

Figure 5. Normal distal biceps. Longitudinal extended-field-of-view US image shows a normal-appearing distal biceps muscle belly *(DB)*, myotendinous junction (∗), and tendon (small arrowheads) at the level of the elbow with distal insertion on the radial tuberosity (large arrowhead). Note the proximity to the brachial artery *(BA)*. *Br* = brachialis, *H* = humerus, *PT* = pronator teres, *R* = radius.

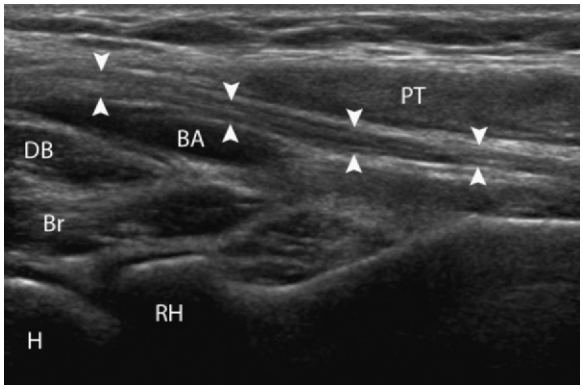

Figure 6. Normal median nerve. Longitudinal US image shows the median nerve (arrowheads) at the level of the elbow. Note the normal fascicular appearance with hypoechoic nerve fascicles and hyperechoic epineurium. The median nerve is medial to the brachial artery *(BA)*. *Br* = brachialis muscle, *DB* = distal biceps, *H* = humerus, *PT* = pronator teres, *RH* = radial head.

tioned slightly inferolaterally, with attention to maintaining the probe parallel to the tendon as it courses obliquely away from the probe to its insertion (8,9). Application of more pressure on the distal half of the transducer ("heel-toe maneuver") aids in maintaining a perpendicular relationship between the ultrasound beam and the DBT. Evaluating the abnormality with various degrees of elbow flexion and extension may help distinguish between anisotropy and tendinopathy or tear (10).

At the level of the elbow joint, the median nerve is located medial to the brachial artery and can be followed distally, coursing between the humeral and ulnar heads of the pronator teres (Figs 4b, 6). The median nerve supplies the pronator teres, flexor carpi radialis, palmaris longus, and flexor digitorum superficialis muscles (11). The median nerve has a characteristic speckled appearance in the short axis as a result of its hypoechoic nerve fascicles and intervening hyperechoic epineurium (10).

Lateral Elbow

The lateral elbow structures to be evaluated include the common extensor tendon, lateral collateral ligamentous complex, radiocapitellar joint, annular recess, capitellum, and radial nerve, including the PIN, which is its deep motor branch (Fig 7). The lateral elbow is evaluated by placing the elbow in flexion with the arm internally rotated (1,10).

To start the examination, the transducer is placed in the coronal plane (longitudinal axis) (Fig 8). Scanning proximally demonstrates the articulation of the radial head with the capitellum; just proximal to this articulation is the lateral epicondyle. With the cranial edge of the transducer on the lateral epicondyle and slightly oblique to the long axis of the upper extremity, the hyperechoic fibrillar pattern of the common extensor tendon origin may be visualized (Fig 9).

The common extensor tendon, the primary extensor of the wrist and hand, is composed of the conjoined tendon (extensor carpi radialis brevis, extensor digitorum communis, and extensor carpi ulnaris) and the extensor digiti minimi. The extensor carpi radialis longus, brachioradialis, and supinator tendons make up the remainder of the extensor mechanism (12,13). Images of the common extensor tendon should be obtained from the hyperechoic triangular origin at the anterior aspect of the lateral epicondyle and lateral supracondylar ridge to its myotendinous junction.

The lateral collateral ligamentous complex provides stability to the lateral elbow joint. It consists of the RCL, annular ligament, and LUCL along with an accessory RCL (1,10). The RCL is a thick band of compact hyperechoic fibers that originates from the inferior lateral epicondyle and inserts on the radius, where it blends with the fibers of the annular ligament (10) (Fig 9).

The LUCL is the major stabilizer against varus stress and posterolateral rotatory stability (14). It originates at the posteroinferior lateral epicondyle deep to the common extensor tendon and posterior to the RCL origin. US of the LUCL is challenging due to its posteromedial curvilinear course as it cradles the radial head to insert on the supinator crest of the proximal ulna. This distinct and tightly fibrillated structure is best evaluated with the transducer placed over the proximal RCL and angled posteriorly toward the ulna (10,15) (Fig 10).

The radial nerve has the characteristic echotexture of a nerve in cross section. Proximally, it

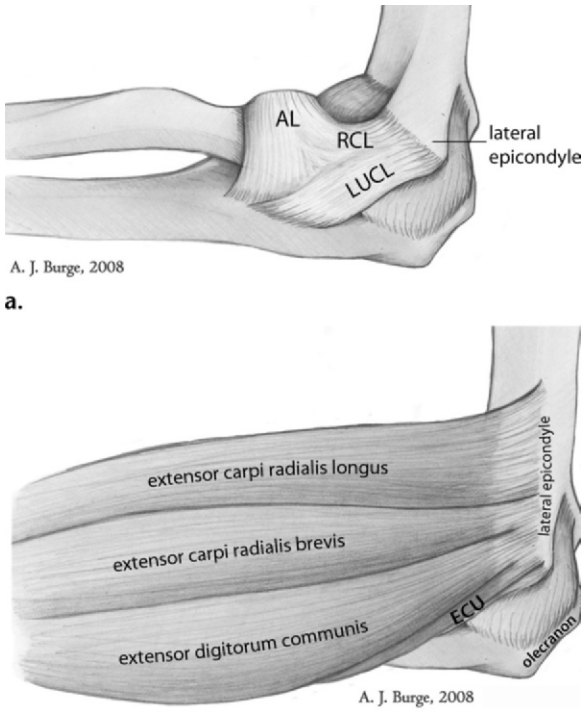

Figure 7. Nomal structures of the lateral elbow. **(a)** Lateral ligaments. *AL* = annular ligament. **(b)** Lateral tendons. The common extensor tendon includes the conjoined tendon (extensor carpi radialis brevis, extensor digitorum communis, and extensor carpi ulnaris *[ECU]*) along with the extensor digiti minimi (not shown but intimately associated with the extensor digitorum communis). The extensor carpi radialis longus, brachioradialis, and supinator tendons make up the remainder of the extensor mechanism (not shown, except for the extensor carpi radialis longus). (Fig 7a and 7b courtesy of Alissa J. Burge, MD, Hospital for Special Surgery, New York, NY.)

Figure 8. Transducer technique for US of the lateral structures of the elbow. The transducer is placed in the coronal plane in the long axis with its cranial aspect over the lateral epicondyle.

a.

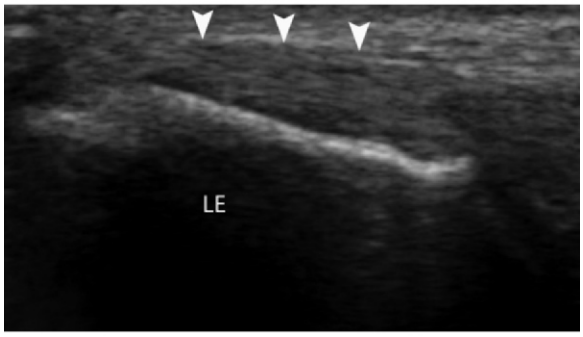

b.

Figure 9. Normal common extensor tendon and RCL. Longitudinal **(a)** and short-axis **(b)** US images show a normal common extensor tendon (arrowheads) originating at the lateral epicondyle *(LE)*. Deep to the common extensor tendon is the RCL (arrows in **a**). *RH* in **a** = radial head.

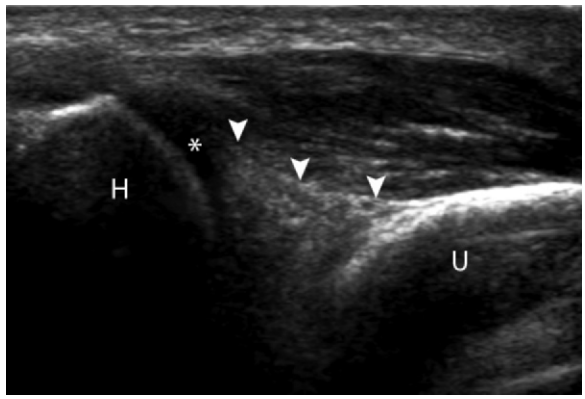

Figure 10. Normal LUCL. US image shows the distal portion of the LUCL (arrowheads) attached to the proximal ulna *(U)*. Anisotropy (∗) is seen at the proximal aspect of the imaged LUCL as it begins to make its curve posteriorly around the radius to its origin at the lateral epicondyle. *H* = humerus.

may be identified over the posterior aspect of the humeral diaphysis, coursing medially to laterally within the spiral groove. It supplies the triceps, anconeus, and brachioradialis muscles and the lateral half of the brachialis muscle (11). At the level of the proximal elbow, the radial nerve is located between the brachioradialis and brachialis muscles.

Teaching Point

At this level, it can be followed to its bifurcation into a superficial sensory branch and a deep motor branch (Fig 11a). The superficial sensory branch courses in the forearm anterior to the brachioradialis muscle. The deep motor branch courses through the radial tunnel; as it exits, it pierces the superficial and deep portions of the supinator muscle as the PIN. At the superficial

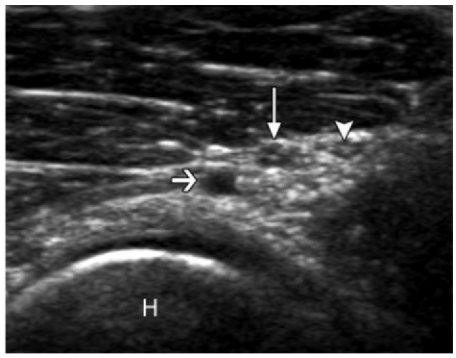

a.

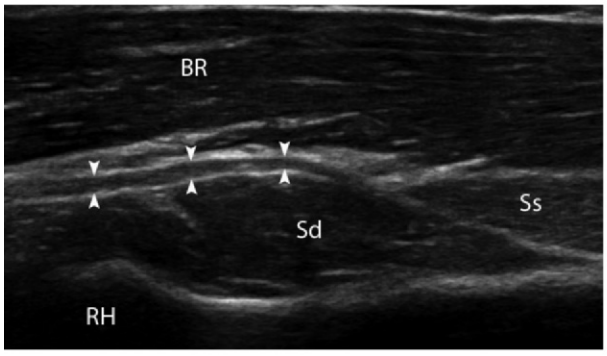

b.

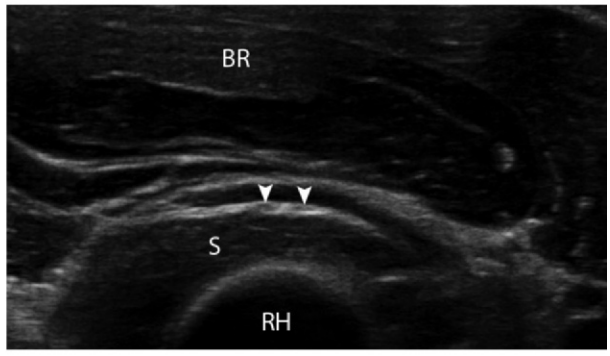

c.

Figure 11. Normal superficial sensory branch and deep motor branch (PIN) of the radial nerve. **(a)** Short-axis US image shows bifurcation of the radial nerve into a superficial sensory branch (arrowhead) and deep motor branch (the PIN) (long arrow). Short arrow = radial artery, *H* = humerus. **(b)** Long-axis US image at the anterolateral proximal forearm shows a normal deep motor branch of the radial nerve or PIN (arrowheads) diving under the arcade of Frohse between the superficial *(Ss)* and deep *(Sd)* heads of the supinator muscle. *BR* = brachioradialis muscle, *RH* = radial head. **(c)** Short-axis US image shows the branches of the PIN (arrowheads) within the supinator muscle *(S)*. *BR* = brachioradialis muscle, *RH* = radial head.

edge of the supinator muscle, there is a fibrous arch—the arcade of Frohse—where entrapment of the PIN may occur as it dives deep to this fibrous bridge (Fig 11b, 11c) (1,16).

To improve evaluation of the PIN, passive pronation and supination of the forearm may be performed while sweeping the probe over the supinator muscle. The deep motor branch at the elbow supplies the extensor carpi radialis brevis and supinator muscles. The PIN supplies the extensor digitorum communis, extensor carpi ulnaris, extensor digiti minimi, abductor pollicis longus and brevis, and extensor indicis proprius muscles (11).

Medial Elbow

Structures of interest in the medial compartment include the common flexor tendon and the anterior band of the UCL (Fig 12). The medial elbow is evaluated with the patient's forearm placed in forceful external rotation and extension or slight flexion (2).

The transducer is placed in the coronal plane (long axis) with its cranial aspect over the medial epicondyle (Fig 13), so that the hyperechoic bony contours of the medial epicondyle and ulnotrochlear articulation will be seen. Further assessment with transverse US may be performed if disease involving the common flexor–pronator mass or anterior band of the UCL is identified.

The common flexor–pronator mass includes the pronator teres and common flexor tendon (flexor carpi radialis, palmaris longus, flexor carpi ulnaris, and flexor digitorum superficialis) and originates at the medial epicondyle of the humerus (13,17). The common flexor tendon primarily functions as a flexor of the wrist and hand, while the pronator teres functions in pronation of the forearm. The pronator teres has two origins, one at the humeral head and the other at the medial coronoid process (13).

The origin of the common flexor–pronator mass has a hyperechoic fibrillar pattern com-

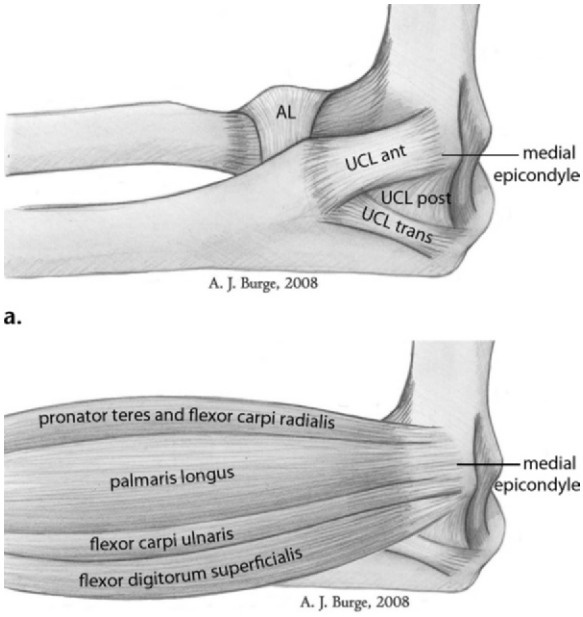

Figure 12. Normal structures of the medial elbow. **(a)** Medial ligaments. *AL* = annular ligament (a lateral structure), *ant* = anterior band (bundle), *post* = posterior band, *trans* = transverse band. **(b)** Common flexor–pronator mass, which includes the pronator teres and common flexor tendon (flexor carpi radialis, palmaris longus, flexor carpi ulnaris, and flexor digitorum superficialis). (Fig 12a and 12b courtesy of Alissa J. Burge, MD, Hospital for Special Surgery, New York, NY.)

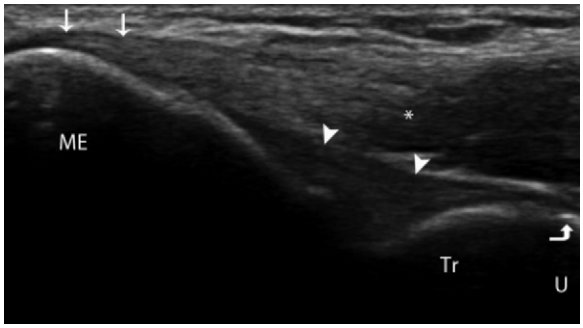

Figure 14. Normal common flexor tendon and UCL. Longitudinal US image shows the hyperechoic fibrillar origin of the common flexor tendon (straight arrows) at the medial epicondyle *(ME)* and the myotendinous junction (*). The common flexor tendon is thicker and shorter than the common extensor tendon. Deep to the common flexor tendon is the slightly more hypoechoic anterior band of the UCL (arrowheads), which extends from the medial epicondyle to the sublime tubercle (curved arrow) on the ulna *(U)*. *Tr* = trochlea.

Figure 13. Transducer technique for US of the medial structures of the elbow. The transducer is placed in the coronal plane (long axis) with its cranial aspect over the medial epicondyle.

parable to that of the common extensor tendon (Fig 14). However, the common flexor–pronator tendon is thicker, shorter, and more easily separated from the joint capsule than the common extensor tendon and has a less broad-based attachment (16,18).

Teaching Point

The UCL is the chief stabilizer of the elbow against valgus stress when it is flexed more than 20°. The UCL consists of three bands (or bundles): anterior, posterior, and oblique. The anterior band or bundle can be divided into two bands, anterior and posterior, and is functionally the most important, as it provides the greatest degree of stabilization (1,19,20).

The normal US appearance of the anterior band is a hyperechoic, thin, compact fibrillar band just deep to the common flexor tendon. It originates from the anteroinferior aspect of the medial epicondyle to insert on the sublime tubercle of the coronoid process of the ulna (Fig 14) (21,22). Variability in the proximal attachment with either a cordlike or broad-based appearance has been described (21,22).

Dynamic US may be performed to evaluate for ligamentous laxity with application of valgus stress on the elbow (22,23). As with all ligaments, the anterior band of the UCL is susceptible to anisotropy.

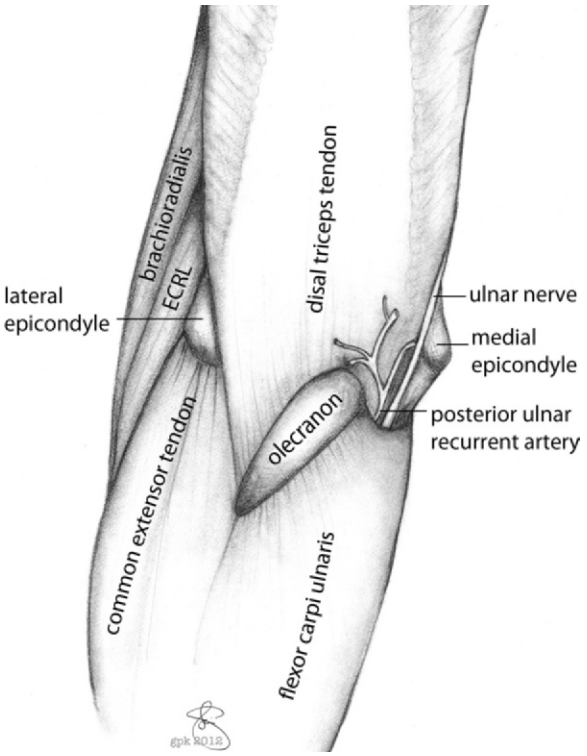

Figure 15. Superficial structures of the posterior elbow. *ECRL* = extensor carpi radialis longus.

Posterior Elbow

The key structures to examine posteriorly include the distal triceps muscle and tendon, posterior joint recess, olecranon bursa, and ulnar nerve within the cubital tunnel (Fig 15). Examination of the posterior elbow is best performed with the joint positioned in 90° of flexion, the forearm fully pronated (internally rotated), and the palm resting on a table ("crab" position) (Fig 16) (2). Alternatively, to evaluate the ulnar nerve, the patient may be supine with the arm abducted, flexed, and internally rotated or prone with the arm adducted by the side and internally rotated.

The examination begins with the transducer placed in the sagittal plane over the proximal elbow posteriorly. The hyperechoic bony contours of the humerus can be evaluated, and the hypoechoic hyaline cartilage of the trochlea and capitellum can be seen. The olecranon fossa is identified as a concavity at the distal aspect of the humerus that is filled with the hyperechoic posterior elbow fat pad (Fig 17). This is the preferred site for evaluation of joint fluid and intraarticular bodies (24). The olecranon bursa is located superficial to the olecranon process and distal triceps tendon and is best interrogated with elbow

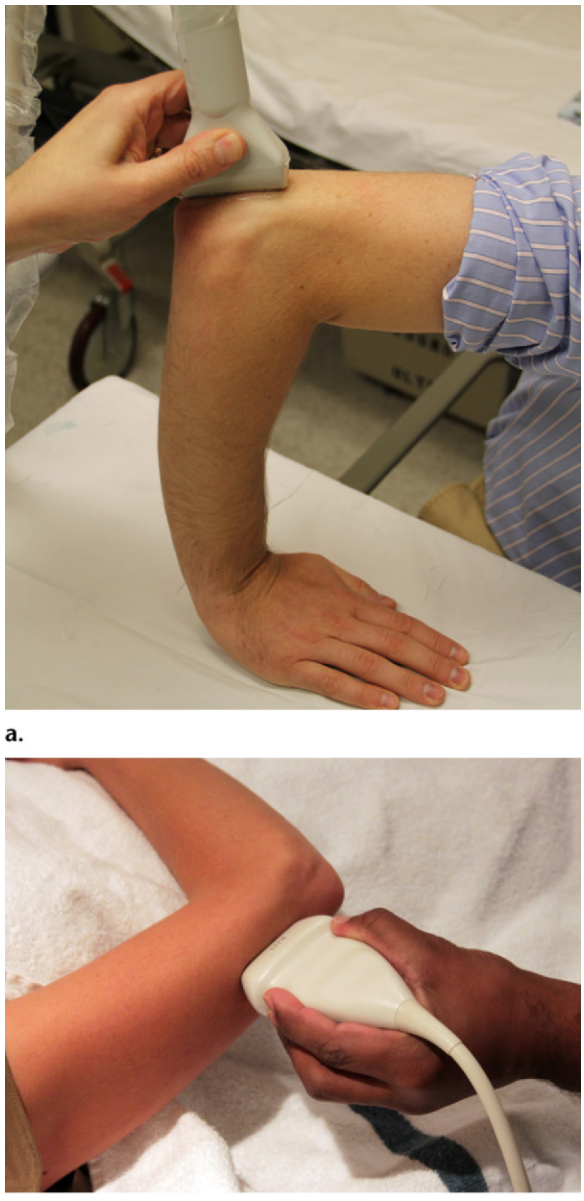

a.

b.

Figure 16. Transducer techniques for US of the posterior elbow. **(a)** Transducer technique with the patient's arm in the crab position. **(b)** Alternate transducer technique with the patient supine and the arm abducted, flexed, and internally rotated.

extension. Use of a thick layer of gel with light transducer pressure will ensure that bursal fluid is not displaced out of the field of view.

The distal triceps muscle consists of three heads—medial, lateral, and long—of which the lateral and long heads converge to form a common tendon that inserts posterior to the insertion of the medial head. The distal triceps tendon inserts approximately 1 cm distal to the apex of the olecranon of the ulna (1). The predominantly hypoechoic triceps muscle and the hyperechoic

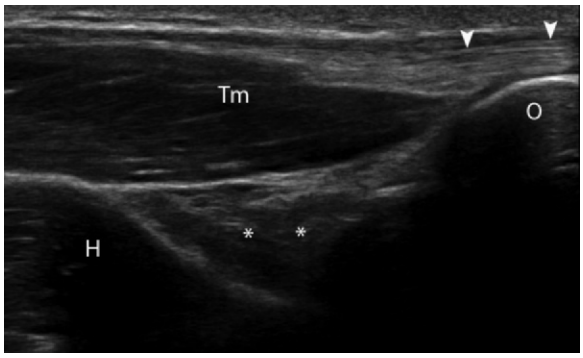

Figure 17. Normal olecranon fossa and distal triceps tendon and muscle. Longitudinal US image shows the normal hypoechoic triceps muscle bellies *(Tm)* and the more hyperechoic fibrillar distal triceps tendon (arrowheads) as it approaches its insertion approximately 1 cm distal to the apex of the olecranon *(O)*. The posterior fat pad (∗) is seen within the olecranon fossa, which is bounded by the echogenic contour of the humerus *(H)*.

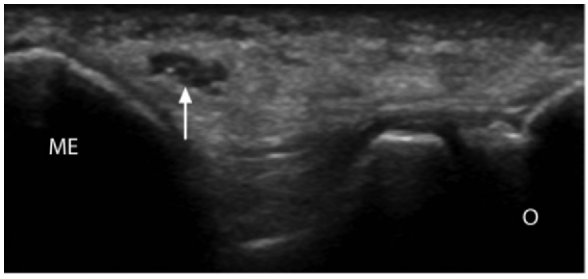

a.

b.

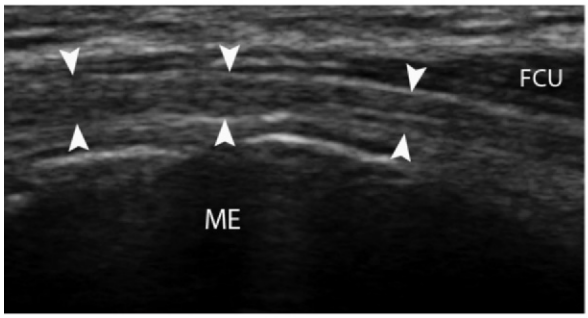

c.

Figure 18. Normal cubital tunnel and ulnar nerve. **(a)** Short-axis US image shows the ulnar nerve (arrow) at the proximal cubital tunnel and its relationship to the medial epicondyle *(ME)*. *O* = olecranon. **(b)** Transverse US image at the distal cubital tunnel, beneath the arcuate ligament (arrowheads), shows the ulnar nerve (arrow) with its characteristic speckled fascicular appearance. The arcuate ligament joins the humeral *(FCUh)* and ulnar *(FCUu)* heads of the flexor carpi ulnaris muscle. **(c)** Longitudinal US image shows a normal ulnar nerve (arrowheads) within the cubital tunnel. *FCU* = flexor carpi ulnaris, *ME* = medial epicondyle.

distal triceps tendon are seen superficial to the olecranon recess and should be evaluated in both short-axis and longitudinal planes (Fig 17). The anconeus muscle arises from the posterior aspect of the lateral epicondyle and inserts on the proximal posterolateral aspect of the ulna. Between the medial epicondyle and medial aspect of the olecranon, a small accessory anconeus epitrochlearis muscle may be identified (1).

The ulnar nerve is found proximally within the cubital tunnel, a fibro-osseous channel formed by the olecranon process laterally, medial epicondyle medially, posterior bundle of the UCL and joint capsule anteriorly, and cubital tunnel retinaculum (Osborne ligament) posteriorly (1). Distally, the ulnar nerve lies deep to the arcuate ligament, an aponeurotic attachment of the two heads of the flexor carpi ulnaris muscle (1). The ulnar nerve supplies the flexor carpi ulnaris and the medial half of the flexor digitorum profundus muscle at the level of the elbow (11).

For optimal evaluation of the cubital tunnel, a large amount of gel should be used with a 10–15-MHz hockey stick probe, if available. The transducer is placed in a transverse plane between the hyperechoic bony protuberances of the olecranon process and medial epicondyle. The fascicular appearance of the ulnar nerve with adjacent hyperechoic fat will be seen within the cubital tunnel and may be followed distally deep to the arcuate ligament (Fig 18).

Teaching Point

Dynamic US of the ulnar nerve should be performed to evaluate for subluxation with or without snapping triceps syndrome (25). With the transducer in the transverse plane between the olecranon process and fixed at the medial epicondyle, the patient is asked to flex the elbow. This maneuver allows assessment of abnormal anterior and medial translation of the ulnar nerve over the medial epicondyle, with or without the medial head of the triceps muscle. It is important

to apply gentle pressure during this dynamic imaging maneuver, so as not to inhibit the abnormal translation of the ulnar nerve.

Tendon and Muscle Disease

DBT Tear or Rupture

DBT tears are much less common than proximal biceps tendon tears, accounting for less than 3% of all biceps tendon tears (26,27). DBT injury typically occurs during eccentric contraction against resistance and as such is common in weight lifters. Typically, patients present with sudden anterior elbow pain and describe a popping sensation while lifting a heavy object. Physical examination reveals weakness of flexion and supination, a palpable defect in the antecubital fossa, and a soft-tissue mass in the upper arm proximally.

Retracted tears do not always require imaging, since they are clinically evident. However, imaging plays an important role in evaluating partial or nonretracted tears due to an intact lacertus fibrosus or when the retracted muscle cannot be palpated due to overlying edema and hemorrhage (8,9). In addition, the degree of tendon retraction may be quantified. Distinction between complete and partial tears is clinically significant, as complete tears are treated surgically and partial tears may be managed conservatively.

Teaching Point

Rupture of the DBT, best visualized in the longitudinal axis, appears as anechoic or hypoechoic discontinuity of tendon fibers with or without retraction and surrounding hypoechoic fluid (9) (Fig 19). With a ruptured lacertus fibrosus, retraction of the tendon often occurs with nonvisualization of the distal tendon. The degree of tendon retraction does not necessarily indicate the status of the lacertus fibrosus (9), and US does not allow reliable visualization of a normal biceps aponeurosis or evidence of its rupture (16). Dynamic US can aid in differentiation of complete from incomplete tears (8,9).

While tendinosis appears as hypoechoic thickening of the tendon (Fig 20), partial tears demonstrate contour waviness, irregularity, and a partial degree of anechoic or hypoechoic disruption of the tendon fibers (9,10). This distinction is somewhat arbitrary in that essentially all patients with tendinosis have degeneration and microtearing. In difficult cases, scanning the normal contralateral elbow may help confirm the tendon abnormality in question by delineating the extent of underlying tendon remodeling.

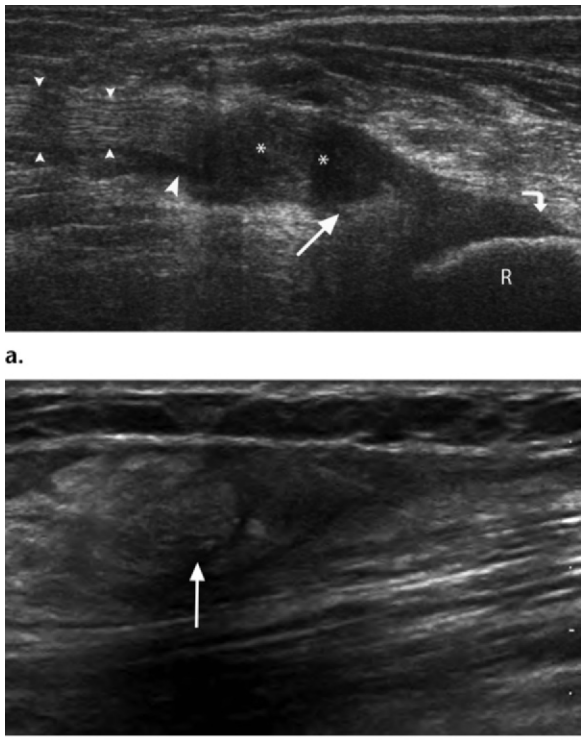

a.

b.

Figure 19. Rupture of the DBT. **(a)** Longitudinal extended-field-of-view US image in a 41-year-old man shows a chronic partial tear of the deep portion of the DBT (straight arrow) with isoechoic granulation tissue filling the gap and a small amount of fluid tracking proximally (large arrowhead). The anterior fibers (curved arrow) remain attached to the radial tuberosity *(R)*. Note the normal fibrillar appearance of the proximal intact DBT (small arrowheads) in contrast to the scar-remodeled tear with amorphous hypoechoic retracted tendon ends (*). **(b)** Long-axis US image in a 20-year-old man shows complete rupture of the right DBT at the level of the myotendinous junction. The balled-up tendon (arrow) was retracted by at least 3 cm proximal to the radial tuberosity.

US evaluation of DBT disease may be limited in less-experienced hands because it is technically challenging. The oblique course of the DBT often results in anisotropy, thus mimicking DBT tendinosis or tear (see the section on the anterior elbow). Demonstration of tendon thickening and hyperemia can help differentiate true tendinopathy from anisotropy. DBT rupture should not be considered without the presence of surrounding fluid or distortion of the imaged soft-tissue

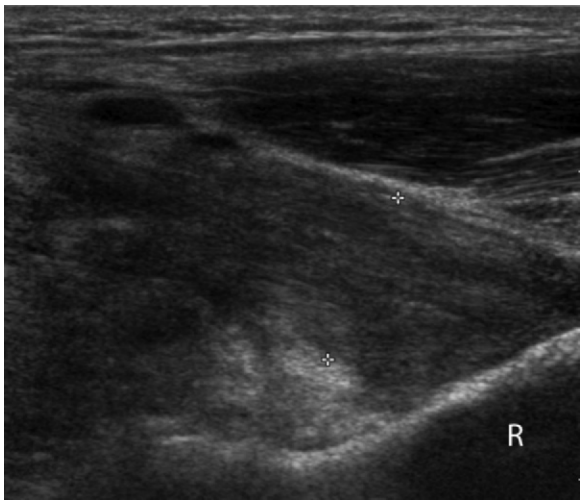

Figure 20. Distal biceps tendinosis in a 38-year-old man who underwent DBT repair. Long-axis US image of the right DBT shows postoperative changes and tendinosis with heterogeneity and marked thickening measuring up to 15 mm (cursors). Restricted motion was demonstrated with dynamic US. *R* = radius.

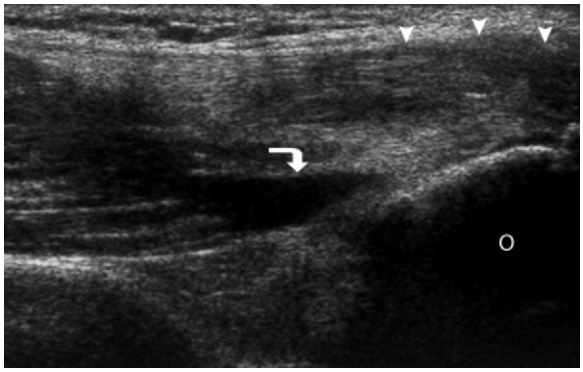

Figure 21. Tear of the distal triceps tendon in a 51-year-old man. Longitudinal US image shows thickening and heterogeneity of the common tendon of the left distal triceps (arrowheads), findings consistent with tendinosis. There is a focal partial tear of the musculotendinous junction of the medial head of the tendon (arrow). *O* = olecranon.

planes (9). Distention of the bicipitoradial bursa may cause difficulty in US evaluation of the DBT. (Bicipitoradial bursitis is discussed in the section on joint and bursa disease.)

Injury of the Distal Triceps Tendon

Distal triceps tendon injuries are uncommon. Local or systemic steroid use, renal disease, and chronic olecranon bursitis are some of the factors predisposing to triceps brachii injury (18). The typical mechanism of injury is eccentric loading of a contracted triceps muscle, such as occurs in a fall on an outstretched hand (16,18). Direct impact is another cause. Clinical diagnosis of distal triceps tendon tears may be limited by extensive pain and swelling, and US can aid in diagnosis and in determining the extent of the tear and the degree of retraction, ultimately allowing more focused management. Partial tears are managed nonsurgically, whereas surgical intervention is reserved for complete tears or incomplete tears with associated loss of strength (28).

Distal triceps tendon tears are frequently avulsive at the tendon-bone interface and may be associated with avulsion fractures of the olecranon process (29). An avulsion fracture will appear as a shadowing hyperechoic focus within the distal triceps tendon along with discontinuity of this fragment with the donor site at the olecranon process. Discontinuity must be differentiated from calcium deposition or enthesopathy within the distal triceps tendon. Disruption of the distal triceps tendon fibers with a fluid gap, retraction, and surrounding fluid indicates a full-thickness tendon tear, whereas partial-thickness tears demonstrate incomplete disruption of the tendon fibers and more commonly involve the posterior common tendon (Fig 21). Longitudinal dynamic scanning during flexion and extension aids in differentiating a partial tear from a nonretracted complete tear. Distal triceps tendinosis appears as hypoechoic expansion of intact fibers.

Epicondylitis

Epicondylitis, more accurately described as tendinosis, is the result of repetitive trauma or overuse, which leads to mucoid degeneration, microtearing, and angiofibroblastic hyperplasia with an immature reparative response (30–32).

Lateral epicondylitis, commonly referred to as "tennis elbow," manifests as localized tenderness at the lateral epicondyle with reduced strength with a resisted grip, supination, and extension at examination. Typically, the anterolateral and middle portions of the common extensor tendon are affected while the posterior portion is spared (15). The extensor carpi radialis brevis tendon of the common extensor tendon is universally involved, followed by the extensor digitorum communis and the remaining tendons and muscles of the extensor mechanism (15,30–32). In general, imaging is not indicated for evaluation of lateral epicondylitis but may be performed in complex, confounding, or recalcitrant cases. US is useful in assessing the severity and extent of tendon abnormality with the advantage of potential guided intervention (32–34). Miller et al (34) demonstrated that US

Teaching Point

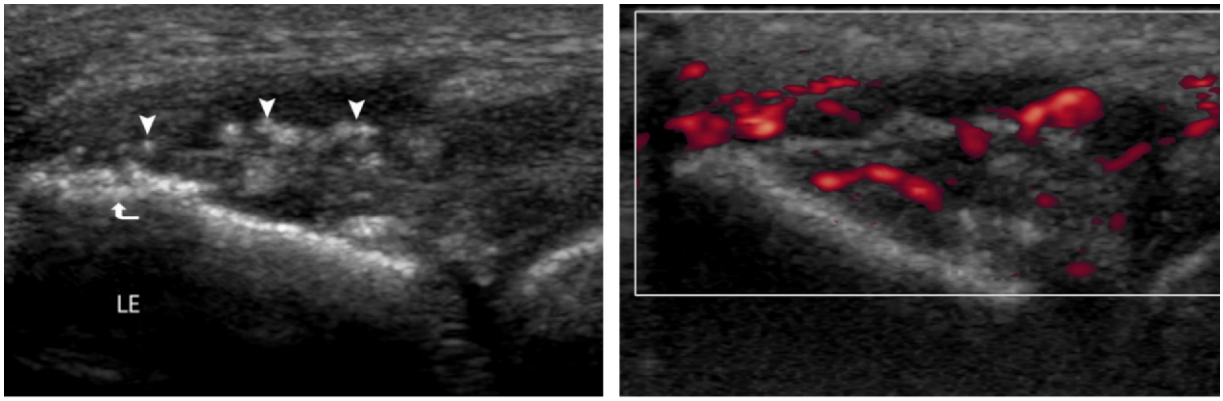

a. b.

Figure 22. Lateral epicondylitis in a 51-year-old woman with severe tendinosis of the right common extensor tendon. **(a)** Longitudinal US image of the common extensor tendon origin shows thickening and marked heterogeneity with numerous hyperechoic calcifications (arrowheads) and hypoechoic intrasubstance tears throughout the tendon, findings consistent with severe chronic tendinosis. Cortical irregularity (arrow) is seen at the lateral epicondyle *(LE)*. **(b)** Longitudinal power Doppler US image shows hyperemia, which is commonly seen in tendinosis.

was as specific as MR imaging but not as sensitive in diagnosis of lateral epicondylitis.

At US, tendinosis can appear as tendon thickening, abnormal or heterogeneous echotexture, or outward bowing of the tendon, possibly with fluid between the tendon and epicondyle (Fig 22a) (33–35). Hyperemia is typical due to the angiofibroblastic response within the tendon (Fig 22b). With surgical and histopathologic correlation, Connell et al (15) showed that tendinopathy appeared sonographically as focal hypoechogenicity or generalized decreased echogenicity, a partial tear appeared as a focal anechoic area with no intact fibers, and a complete tear appeared as a discrete cleavage plane traversing the full width of the common extensor tendon origin. Recognition of anisotropy is important when evaluating the extensor carpi radialis brevis origin so as not to mistake a focus of hypoechogenicity for tendinopathy or a partial tear. Intratendinous calcification or enthesopathy may be present in cases of chronic tendinosis (15,33).

The LUCL, which lies immediately deep to the extensor carpi radialis brevis, should be assessed if possible. If injured, the LUCL may be the source of failure of treatment for lateral epicondylitis (14). If the LUCL is injured and the patient undergoes surgery with release of the common extensor tendon, further destabilization with posterolateral rotatory instability may occur (36).

Medial epicondylitis, commonly referred to as "golfer's elbow," manifests as insidious medial elbow pain with exacerbation by grasping and resistance on wrist flexion and forearm pronation. The flexor carpi radialis and pronator teres, which attach anteriorly at the medial epicondyle, are primarily affected in medial epicondylitis (17). As with lateral epicondylitis, chronic overuse and microtearing ultimately lead to degeneration and angiofibroblastic change with an inadequate reparative response (30–32). The US appearance of medial epicondylitis is similar to that of the more common lateral epicondylitis (Fig 23).

Treatment options are similar for both medial and lateral epicondylitis. Most patients improve with conservative treatment including icing, antiinflammatory medication, corticosteroid injections, splinting, or physical therapy. Alternative therapy includes percutaneous tenotomy (dry needling) with or without platelet-rich plasma injection, prolotherapy, or extracorporeal shock wave lithotripsy (13,32,37). Surgery may be considered in cases refractory to more conservative measures.

Ligamentous Disease

UCL Injury

The anterior band of the UCL, the major stabilizer of the elbow joint to valgus stress, may be

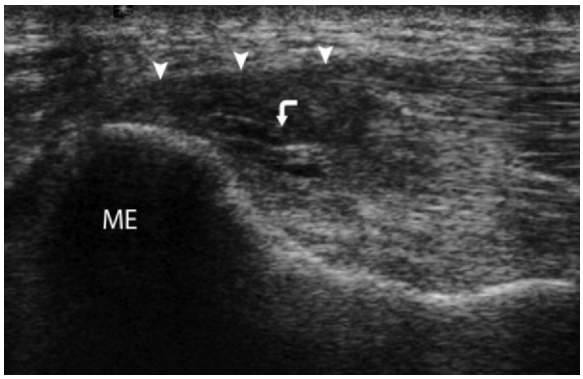

Figure 23. Medial epicondylitis in a 60-year-old man with severe tendinosis of the common flexor–pronator mass origin. Long-axis US image shows marked thickening, hypoechogenicity, and heterogeneity at the origin of the right common flexor–pronator mass (arrowheads) with numerous anechoic intrasubstance tears (arrow). *ME* = medial epicondyle.

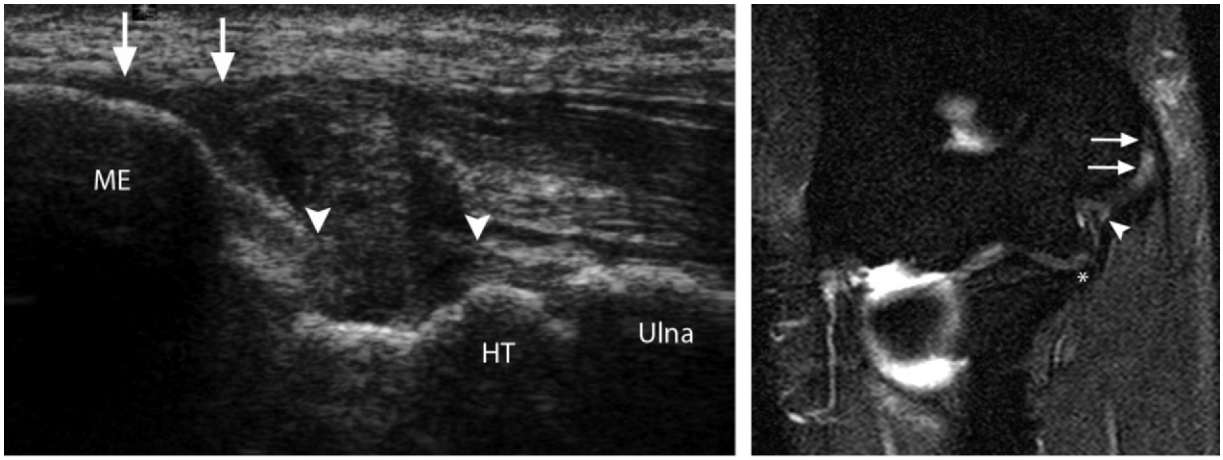

a. **b.**

Figure 24. Near full-thickness chronic tear of the UCL in a 29-year-old right-handed professional baseball pitcher. **(a)** Longitudinal US image shows a partial-thickness, chronic remodeled tear of the proximal UCL with a hypoechoic scar-in-continuity (arrowheads). Dynamic US with application of valgus stress demonstrated an abnormal stress response. Excessive valgus force imparted by throwing often results in UCL instability with coexistent injury to the common flexor–pronator mass (arrows). The partial-thickness UCL tear and medial epicondylitis were confirmed at MR imaging. *HT* = humeral trochlea, *ME* = medial epicondyle. **(b)** Coronal fat-saturated T2-weighted MR image shows a partial-thickness proximal tear of the anterior band of the UCL (arrowhead). The distal insertion at the sublime tubercle is intact (*). Degeneration with low-grade partial undersurface tearing affects the common flexor–pronator origin (arrows).

injured acutely or more commonly from chronic repetitive microtrauma, as occurs in baseball pitchers during the late cocking and early acceleration phases of throwing (17,19,20,23). The UCL is often injured concomitantly with the overlying common flexor–pronator mass (17,32).

A partial tear of the UCL appears as focal hypoechoic heterogeneity and ligamentous thickening (21,23). Disruption of the UCL with widening of the ulnotrochlear joint indicates a full-thickness tear (Fig 24). Differentiation between complete and incomplete tears is often difficult, but dynamic imaging with valgus stress allows functional assessment of the UCL by demonstrating joint instability (23). Valgus stress applied to the elbow joint allows assessment of ligamentous laxity, which is determined by the degree of ulnohumeral joint space widening (Movie 1 [online]).

Evaluation of the contralateral UCL is advantageous, as it provides useful information about the normal appearance of the UCL and the inherent stability of the patient's ulnohumeral joint. Conservative therapy is generally advocated as a first-line treatment. However, for high-level throwing athletes such as professional baseball pitchers with impaired function and a UCL tear, reconstructive surgery may be indicated (23).

LUCL and RCL Injury

Laterally, the LUCL and RCL should be assessed. Tears of these two ligaments have a sonographic appearance similar to that described earlier for UCL tears.

Deficiency of the LUCL may result in posterolateral rotatory instability of the joint with varus stress (Fig 25). It is important to diagnose LUCL tears preoperatively in cases of lateral epicondylitis, otherwise treatment failure including worsening of symptoms and posterolateral rotatory instability may occur (14). Dynamic imaging with hand supination and pronation should be performed to evaluate for LUCL injury and abnormal radial head movement (10). However, evaluation of the LUCL is often difficult and MR imaging may be indicated, as it is a more sensitive modality. The RCL is also intimately associated with the common extensor tendon and should be carefully assessed in cases of lateral epicondylitis (Fig 26).

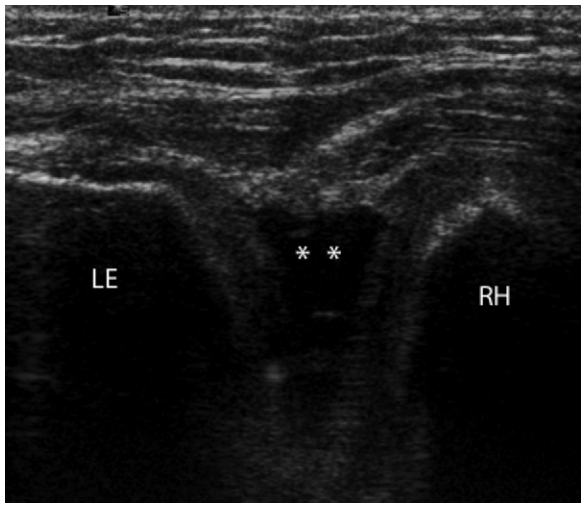

Figure 25. Tear of the LUCL in a 59-year-old man. Longitudinal US image shows a hypoechoic fluid-filled gap (*) that represents a tear of the LUCL. *LE* = lateral epicondyle, *RH* = radial head.

Joint and Bursa Disease

Joint Effusion

An elbow joint effusion is readily amenable to US detection with fluid distention of the anterior or posterior joint recesses (Fig 27). Imaging the posterior joint in flexion is the most sensitive means by which one can demonstrate joint fluid (5). Small adjustments in elbow joint position redistribute the joint fluid and may help detect a joint effusion. With the transducer in the sagittal plane, displacement of the posterior fat pad superiorly and posteriorly will be appreciated.

Joint effusions may be simple and anechoic or complex containing internal echogenicity, the latter of which may indicate infection, hemorrhage, or debris related to small intraarticular bodies or inflammation (18). It is essential to recognize septic arthritis early to avoid irreversible joint destruction and loss of joint function. Although MR imaging is most sensitive for detection of small joint effusions (5), US has the advantage of direct guided visualization for joint aspiration.

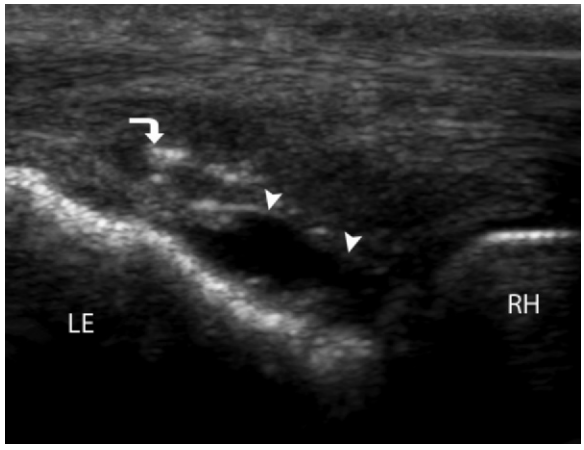

Figure 26. Full-thickness tear of the RCL in a 75-year-old man. Long-axis US image shows a full-thickness tear of the right RCL as a hypoechoic fluid-filled gap (arrowheads). Overlying chronic calcific tendinosis of the common extensor tendon is seen (arrow). *LE* = lateral epicondyle, *RH* = radial head.

Synovitis

Synovitis can distend the joint recesses and should be differentiated from a simple joint effusion. Graded compression without motion of joint contents or displacement of fluid and increased blood flow at color or power Doppler US are indicative of synovitis rather than a joint effusion (1,10,18). Synovitis may be the result

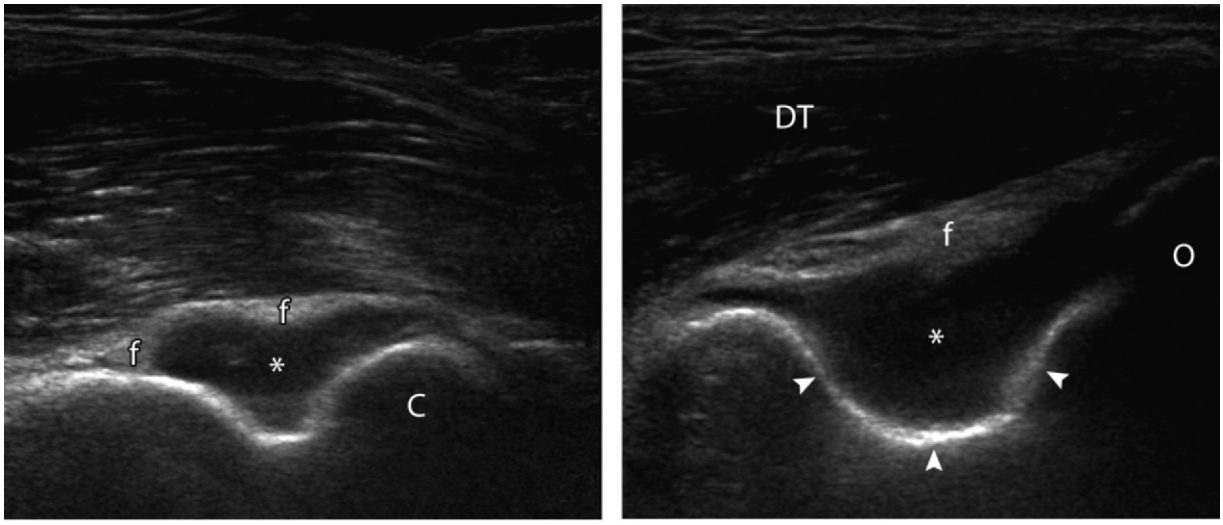

a. b.

Figure 27. Anterior and posterior joint effusions in a 49-year-old man. **(a)** Longitudinal US image shows anechoic fluid (*) filling the left coronoid fossa with elevation of the hyperechoic joint capsule and anterior fat pads *(f)*. *C* = capitellum. **(b)** Longitudinal US image shows anechoic fluid (*) filling the left olecranon fossa (arrowheads) with elevation of the hyperechoic joint capsule and posterior fat pad *(f)*. *DT* = distal triceps tendon, *O* = olecranon.

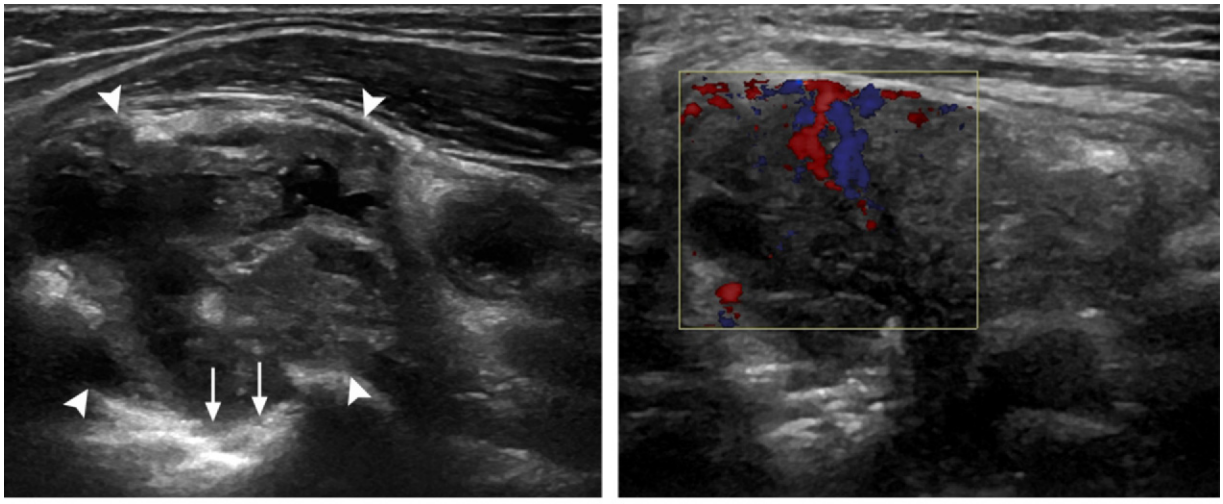

a. b.

Figure 28. Rheumatoid arthritis in a 61-year-old man with active synovitis. Transverse gray-scale **(a)** and color Doppler **(b)** US images of the left anterior elbow joint show marked pannus formation (arrowheads in **a**) with moderate hyperemia. Subjacent to the pannus are numerous osseous erosions (arrows in **a**).

of inflammation from chronic osteoarthrosis, inflammatory arthropathy (eg, rheumatoid arthritis, gout, pseudogout), or infection. Pannus appears as hyperemic synovial thickening of variable echogenicity, as seen in patients with rheumatoid arthritis (Fig 28). Synovial proliferative disorders may be assessed as well, including pigmented villonodular synovitis or synovial osteochondromatosis, of which the latter will be seen as multiple similar-sized hyperechoic foci within the synovial fluid.

Intraarticular Bodies

Assessing for the presence of intraarticular bodies is important, as the elbow is the second most common site of intraarticular bodies after the knee (16). The olecranon, coronoid, and annular recesses are common sites for intraarticular bodies. Visualization of a fragment surrounded by hypoechoic fluid allows identification of an intraarticular location (Fig 29). Ossified and nonossified fragments will appear hyperechoic and can demonstrate shadowing.

The appearance of shifting fluid and small intraarticular bodies can be accentuated by a gentle rocking motion of the patient's elbow (38). Intraarticular injection of sterile saline in a patient suspected of having occult intraarticular bodies without a joint effusion can assist in their identification (39). It is important to evaluate the capitellum carefully for a defect in the articular hyaline cartilage, as it is a common donor site of intraarticular bodies.

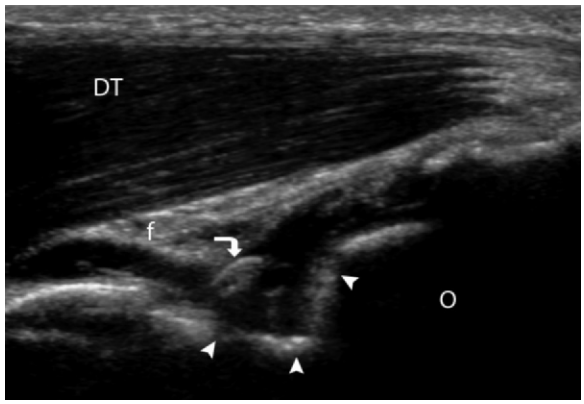

Figure 29. Intraarticular bodies in a 19-year-old man after a football injury. Long-axis US image shows a curvilinear hyperechoic intraarticular body (arrow) with surrounding moderate anechoic joint effusion in the olecranon fossa (arrowheads) and posterior displacement of the posterior fat pad *(f)*. *DT* = distal triceps tendon, *O* = olecranon.

Bursitis

The bursae about the elbow joint include the olecranon, bicipitoradial, and interosseous bursae. Bursitis can result from an inflammatory arthropathy, infection, trauma, synovial proliferative disease, or more commonly repetitive mechanical trauma. Normal bursae are not visualized sonographically but are easily seen when distended with fluid, which may be septated and demonstrate variable echogenicity.

Color and power Doppler US may show increased flow within the bursal lining. Findings similar to those described for the joint recesses may be applied to determine the nature of the bursal distention. It is important not to apply excessive pressure to avoid displacing small effusions out of the bursal collection. Well-defined borders and a characteristic location help differentiate a bursal collection from a joint effusion or abscess.

The olecranon bursa, the most common elbow bursa to be affected, is located superficial to the olecranon process. Olecranon bursitis is most commonly caused by localized repetitive trauma (Fig 30). The bicipitoradial bursa can become distended with bursal fluid lateral to the DBT attachment and anterior to the radius (Fig 31). An enlarged bicipitoradial bursa may compress the deep motor branch of the radial nerve, leading to motor symptoms, a condition known as cubital bursitis (40).

Bicipitoradial bursitis may mimic synovial or ganglion cysts or other soft-tissue masses; however, the typical horseshoe shape of the bicipitoradial bursa as it wraps around the DBT can be a helpful distinguishing feature. Tenosynovitis should not be included in the differential diagnosis, as there is a paratenon rather than a tendon sheath at the distal biceps brachii tendon. Bursitis can be treated with US-guided aspiration or corticosteroid administration.

Peripheral Nerve Disease

Ulnar Nerve

At the elbow, the ulnar nerve is subject to trauma or entrapment at two main sites: *(a)* At the level of the olecranon process and medial epicondyle, the ulnar nerve enters the cubital tunnel and passes beneath the Osborne ligament, where it may be affected by acute trauma, overuse injury, nerve

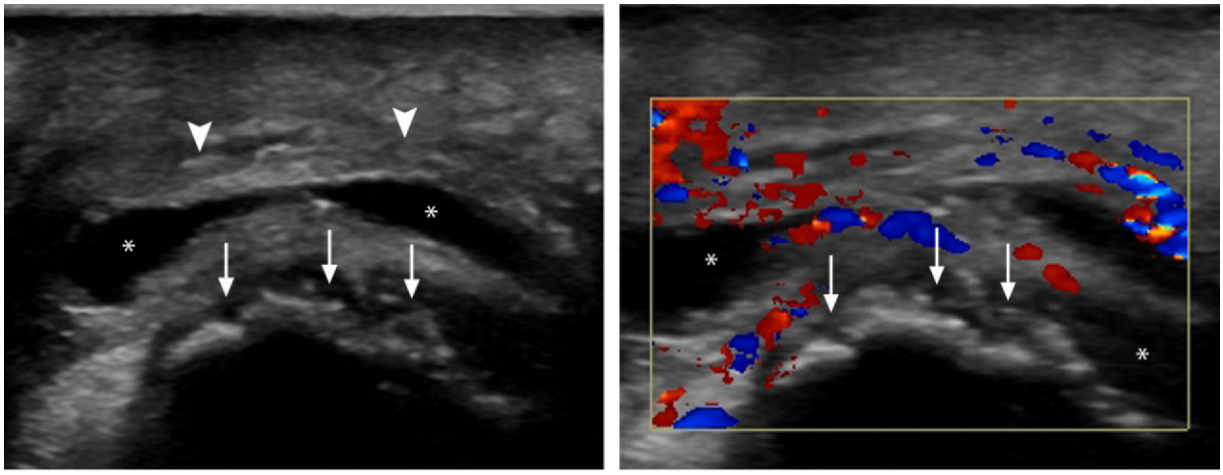

a. b.

Figure 30. Olecranon bursitis secondary to gout in a 50-year-old man. **(a)** Transverse US image shows a complex hypoechoic fluid collection (∗) with synovial thickening (arrowheads) and cortical irregularity with hyperechoic foci (arrows), which are consistent with osseous erosions and crystalline deposition from gout. **(b)** Color Doppler image shows hyperemic synovium. ∗ = complex hypoechoic fluid collection, arrows = osseous erosions and crystalline deposition from gout.

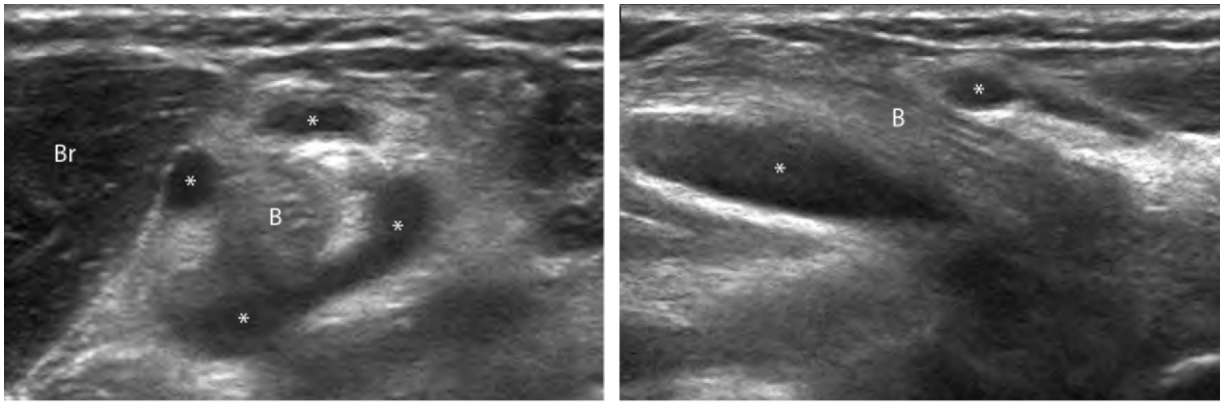

a. b.

Figure 31. Bicipitoradial bursitis in a 72-year-old man. Transverse **(a)** and long-axis **(b)** US images show a distended right bicipitoradial bursa (∗) surrounding the DBT *(B)*. *Br* in **a** = brachialis muscle.

subluxation due to laxity of the cubital retinaculum, or compression, as occurs with an anomalous anconeus epitrochlearis muscle, a hypertrophied medial triceps muscle, or an accessory head of the triceps muscle (1,10,11). *(b)* The ulnar nerve may also be compressed more distally, at the level of the dual origin of the flexor carpi ulnaris, which is bridged by the arcuate ligament (1,16).

Although clinical examination and electrophysiologic studies are usually diagnostic for neuropathies, US allows diagnosis of ulnar nerve entrapment (cubital tunnel syndrome) by demonstrating a hypoechoic thickened ulnar nerve with a cross-sectional area greater than 7.5 mm^2 at

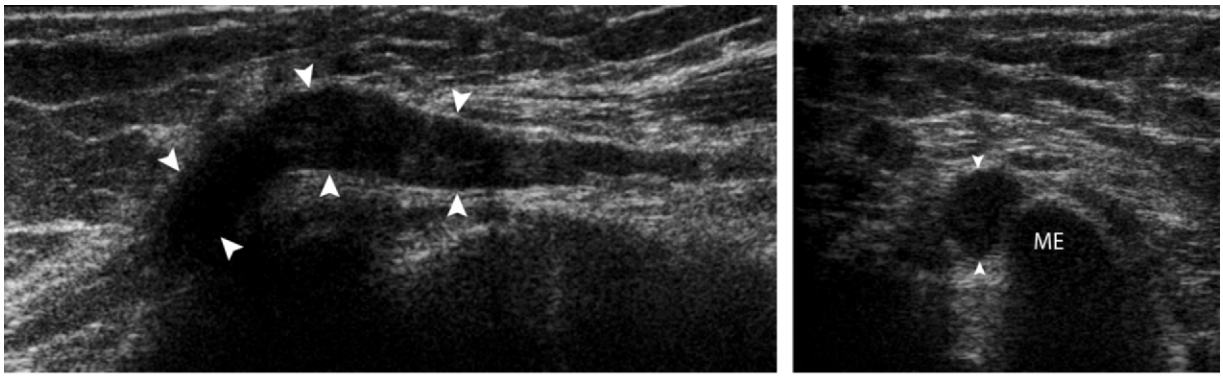

a. b.

Figure 32. Severe cubital tunnel syndrome in a 39-year-old woman. Longitudinal **(a)** and short-axis **(b)** US images at the level of the left cubital tunnel show marked enlargement of the ulnar nerve (arrowheads), which measures up to 40 mm^2 with tapering at the ligament of Osborne, findings consistent with severe cubital tunnel syndrome. *ME* in **b** = medial epicondyle.

Figure 33. Entrapment of the PIN in a 72-year-old man. Long-axis US image of the left PIN (deep motor branch of the radial nerve) (arrowheads) shows focal hypoechoic enlargement of the nerve (arrow) just proximal to the arcade of Frohse. *Sd* = deep supinator muscle, *Ss* = superficial supinator muscle.

the level of the medial epicondyle (25,41) (Fig 32). Alternatively, a ratio of the cross-sectional area at the location of maximal nerve swelling to the cross-sectional area at a nonenlarged location may be most useful. Surgical treatment options include ulnar nerve decompression, which includes cubital tunnel release with an incision through both the Osborne ligament and the arcuate ligament or, more commonly, transposition of the ulnar nerve. Ulnar nerve transposition places the nerve anterior to the medial epicondyle and typically superficial to the flexor muscles (1).

A thickened, hypoechoic ulnar nerve with loss of its fascicular appearance may be seen in ulnar nerve subluxation as a result of irritation from friction during translocation. Furthermore, a subluxated ulnar nerve is vulnerable to direct injury. Subluxation of the ulnar nerve is thought to occur in the absence of the Osborne ligament (42,43). A snapping sensation with elbow flexion is commonly palpated at physical examination. Dynamic imaging during active elbow flexion will demonstrate medial and anterior dislocation of the ulnar nerve over the medial epicondyle (Movie 2 [online]). Typically, the ulnar nerve will relocate within the cubital tunnel during elbow extension. Correlation with symptoms and the appearance of the contralateral nerve is important, as ulnar nerve subluxation is seen in up to 20% of asymptomatic patients (1,25). Ulnar nerve transposition is a potential treatment option for symptomatic ulnar nerve subluxation.

Snapping triceps syndrome should be assessed concomitantly with ulnar nerve subluxation. If a snapping triceps is not diagnosed and treated before ulnar nerve transposition surgery, symptoms

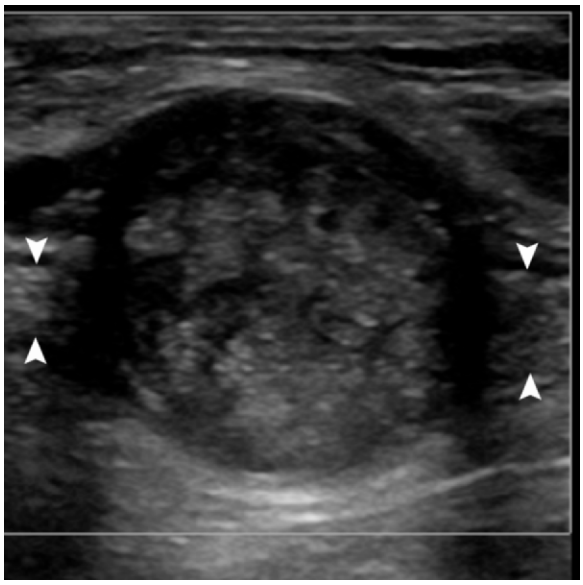

Figure 34. Median nerve schwannoma. Longitudinal US image shows a circumscribed, fusiform mass with mixed echogenicity along the course of the median nerve. The proximal and distal portions of the median nerve are seen (arrowheads). Color Doppler US showed no appreciable vascularity.

will persist (25) (Movie 3 [online]). Snapping triceps syndrome is thought to be due to both congenital and acquired causes (eg, weight lifting) (25). At physical examination, there will be two palpable snaps as opposed to the one snap seen with isolated ulnar nerve dislocation. Dislocation of the medial head of the triceps muscle and the ulnar nerve over the medial epicondyle during elbow flexion is diagnostic and is readily assessed with dynamic imaging (1,16,25) (Movie 4 [online]).

Median Nerve

The median nerve may be subject to entrapment at several sites along the anteromedial aspect of the elbow joint. Entrapment may occur at the anterior distal humerus due to the ligament of Struthers, which extends from a bony excrescence (the supracondylar process) to the medial epicondyle (16), or due to a thickened biceps muscle. Pronator teres hypertrophy is the most common cause of median nerve entrapment as the nerve travels between the superficial and deep heads of the pronator teres muscle. Finally, within the proximal forearm, a thickened proximal edge of the flexor digitorum superficialis muscle may result in entrapment (10,11,16). The anterior interosseous nerve, a branch of the median nerve, may be entrapped distally by fibrous bands, masses, or hypertrophied or anomalous muscles (10).

Radial Nerve

Radial nerve entrapment may involve the superficial branch of the nerve, resulting in sensory symptoms, or the deep motor branch of the nerve (the PIN), leading to weak extensor muscles (44). Posterior interosseous neuropathy may be due to entrapment of the nerve at the arcade of Frohse or to a soft-tissue mass, such as an enlarged bicipitoradial bursa or cyst. Entrapment of the PIN results in abnormal hypoechoic thickening of the involved nerve (Fig 33). Fractures of the radial head or neck or posttraumatic scar tissue may result in compression or stretching injuries of the PIN (1).

Peripheral Nerve Sheath Tumors

Other peripheral nerve abnormalities to consider, not specific to the nerves about the elbow, include peripheral nerve sheath tumors such as schwannomas and neurofibromas. These entities are typically homogeneous and hypoechoic and demonstrate posterior acoustic enhancement (45). Peripheral nerve continuity is a key feature because it significantly limits the differential diagnosis to a peripheral nerve sheath tumor (45) (Fig 34). Internal blood flow at color Doppler imaging may be helpful in distinguishing a peripheral nerve sheath tumor from a ganglion cyst, which usually lacks internal blood flow but demonstrates a similar hypoechoic appearance and posterior acoustic enhancement.

Miscellaneous Conditions

Epitrochlear Lymphadenitis

Epitrochlear nodes provide lymphatic drainage of the forearm and are located at the medial aspect of the elbow, just proximal to the medial epicondyle. A normal lymph node is reniform in shape. At US, it demonstrates increased central echogenicity indicative of fat.

An abnormally enlarged and round lymph node is classically associated with cat-scratch disease, which manifests clinically as a tender, palpable mass at the medial elbow (46). Other possible causes that should be considered in the differential diagnosis of an abnormal lymph node include malignancy, sarcoidosis, lymphoma, and reactive inflammation from a distal inflammatory or infectious process (10).

Bone Abnormalities

Dynamic scanning with passive pronation and supination of the forearm may help one visualize fractures of the radial head. At US, an acute fracture will appear as cortical discontinuity or a step-off deformity (47). Furthermore, radiocapitellar arthropathy and osteochondral lesions of the capitellum can be detected with US (48). The annular ligament may be assessed with this same maneuver (2). For this reason, in children, US can aid in evaluation of "pulled arm" (nursemaid's elbow) (49,50).

Conclusion

US is an excellent diagnostic imaging modality for a wide array of abnormalities affecting the elbow. Although US can be technically challenging, it has diagnostic value as an important real-time and dynamic adjunct or alternative to MR imaging. The ability to perform guided intervention further enhances its value as a clinical tool. The radiologist should be familiar with proper US technique, normal elbow anatomy, and common pathologic conditions of the elbow.

References

1. Bianchi S, Martinoli C. Elbow. In: Bianchi S, Martinoli C, eds. Ultrasound of the musculoskeletal system. New York, NY: Springer, 2007; 349–408.
2. Beggs I, Bianchi S, Bueno A, et al. Musculoskeletal ultrasound technical guidelines. II. Elbow. European Society of Musculoskeletal Radiology, 2006. http://www.essr.org/html/img/pool/elbow.pdf. Accessed January 2012.
3. Hogan MJ, Rupich RC, Bruder JB, Barr LL. Age-related variability in elbow joint capsule thickness in asymptomatic children and adults. J Ultrasound Med 1994;13(3):211–213.
4. Miles KA, Lamont AC. Ultrasonic demonstration of the elbow fat pads. Clin Radiol 1989;40(6):602–604.
5. De Maeseneer M, Jacobson JA, Jaovisidha S, et al. Elbow effusions: distribution of joint fluid with flexion and extension and imaging implications. Invest Radiol 1998;33(2):117–125.
6. Skaf AY, Boutin RD, Dantas RWM, et al. Bicipitoradial bursitis: MR imaging findings in eight patients and anatomic data from contrast material opacification of bursae followed by routine radiography and MR imaging in cadavers. Radiology 1999;212(1):111–116.
7. Dirim B, Brouha SS, Pretterklieber ML, et al. Terminal bifurcation of the biceps brachii muscle and tendon: anatomic considerations and clinical implications. AJR Am J Roentgenol 2008;191(6):W248–W255.
8. Chew ML, Giuffrè BM. Disorders of the distal biceps brachii tendon. RadioGraphics 2005;25(5):1227–1237.
9. Miller TT, Adler RS. Sonography of tears of the distal biceps tendon. AJR Am J Roentgenol 2000;175(4):1081–1086.
10. Jacobson JA. Fundamentals of musculoskeletal ultrasound. Philadelphia, Pa: Saunders Elsevier, 2007.
11. Miller TT, Reinus WR. Nerve entrapment syndromes of the elbow, forearm, and wrist. AJR Am J Roentgenol 2010;195(3):585–594.
12. Bunata RE, Brown DS, Capelo R. Anatomic factors related to the cause of tennis elbow. J Bone Joint Surg Am 2007;89(9):1955–1963.
13. Blease S, Stoller DW, Safran MR, Li AE, Fritz RC. The elbow. In: Stoller DW, ed. Magnetic resonance imaging in orthopaedics and sports medicine. 3rd ed. Philadelphia, Pa: Lippincott, Williams & Wilkins, 2007; 1463–1626.
14. Bredella MA, Tirman PF, Fritz RC, Feller JF, Wischer TK, Genant HK. MR imaging findings of lateral ulnar collateral ligament abnormalities in patients with lateral epicondylitis. AJR Am J Roentgenol 1999;173(5):1379–1382.
15. Connell D, Burke F, Coombes P, et al. Sonographic examination of lateral epicondylitis. AJR Am J Roentgenol 2001;176(3):777–782.
16. Martinoli C, Bianchi S, Giovagnorio F, Pugliese F. Ultrasound of the elbow. Skeletal Radiol 2001;30(11):605–614.
17. Ciccotti MC, Schwartz MA, Ciccotti MG. Diagnosis and treatment of medial epicondylitis of the elbow. Clin Sports Med 2004;23(4):693–705, xi.
18. Finlay K, Ferri M, Friedman L. Ultrasound of the elbow. Skeletal Radiol 2004;33(2):63–79.

19. Morrey BF, An KN. Articular and ligamentous contributions to the stability of the elbow joint. Am J Sports Med 1983;11(5):315–319.
20. Schwab GH, Bennett JB, Woods GW, Tullos HS. Biomechanics of elbow instability: the role of the medial collateral ligament. Clin Orthop Relat Res 1980;146(146):42–52.
21. Jacobson JA, Propeck T, Jamadar DA, Jebson PJ, Hayes CW. US of the anterior bundle of the ulnar collateral ligament: findings in five cadaver elbows with MR arthrographic and anatomic comparison—initial observations. Radiology 2003;227(2):561–566.
22. Ward SI, Teefey SA, Paletta GA Jr, et al. Sonography of the medial collateral ligament of the elbow: a study of cadavers and healthy adult male volunteers. AJR Am J Roentgenol 2003;180(2):389–394.
23. Nazarian LN, McShane JM, Ciccotti MG, O'Kane PL, Harwood MI. Dynamic US of the anterior band of the ulnar collateral ligament of the elbow in asymptomatic major league baseball pitchers. Radiology 2003;227(1):149–154.
24. Fessell DP, Jacobson JA, Craig J, et al. Using sonography to reveal and aspirate joint effusions. AJR Am J Roentgenol 2000;174(5):1353–1362.
25. Jacobson JA, Jebson PJ, Jeffers AW, Fessell DP, Hayes CW. Ulnar nerve dislocation and snapping triceps syndrome: diagnosis with dynamic sonography—report of three cases. Radiology 2001;220(3):601–605.
26. Agins HJ, Chess JL, Hoekstra DV, Teitge RA. Rupture of the distal insertion of the biceps brachii tendon. Clin Orthop Relat Res 1988;234(234):34–38.
27. Bourne MH, Morrey BF. Partial rupture of the distal biceps tendon. Clin Orthop Relat Res 1991;271(271):143–148.
28. Yeh PC, Dodds SD, Smart LR, Mazzocca AD, Sethi PM. Distal triceps rupture. J Am Acad Orthop Surg 2010;18(1):31–40.
29. Kaempffe FA, Lerner RM. Ultrasound diagnosis of triceps tendon rupture: a report of 2 cases. Clin Orthop Relat Res 1996;332(332):138–142.
30. Nirschl RP, Pettrone FA. Lateral and medial epicondylitis. In: Morrey BF, ed. Master techniques in orthopedic surgery: the elbow. New York, NY: Raven, 1994; 537–552.
31. Potter HG, Hannafin JA, Morwessel RM, DiCarlo EF, O'Brien SJ, Altchek DW. Lateral epicondylitis: correlation of MR imaging, surgical, and histopathologic findings. Radiology 1995;196(1):43–46.
32. Walz DM, Newman JS, Konin GP, Ross G. Epicondylitis: pathogenesis, imaging, and treatment. RadioGraphics 2010;30(1):167–184.
33. Levin D, Nazarian LN, Miller TT, et al. Lateral epicondylitis of the elbow: US findings. Radiology 2005;237(1):230–234.
34. Miller TT, Shapiro MA, Schultz E, Kalish PE. Comparison of sonography and MRI for diagnosing epicondylitis. J Clin Ultrasound 2002;30(4):193–202.
35. Maffulli N, Regine R, Carrillo F, Capasso G, Minelli S. Tennis elbow: an ultrasonographic study in tennis players. Br J Sports Med 1990;24(3):151–155.
36. Nirschl RP, Pettrone FA. Tennis elbow: the surgical treatment of lateral epicondylitis. J Bone Joint Surg Am 1979;61(6A):832–839.
37. Louis LJ. Musculoskeletal ultrasound intervention: principles and advances. Radiol Clin North Am 2008;46(3):515–533, vi.
38. Bianchi S, Martinoli C. Detection of loose bodies in joints. Radiol Clin North Am 1999;37(4):679–690.
39. Miller JH, Beggs I. Detection of intraarticular bodies of the elbow with saline arthrosonography. Clin Radiol 2001;56(3):231–234.
40. Sofka CM, Adler RS. Sonography of cubital bursitis. AJR Am J Roentgenol 2004;183(1):51–53.
41. Chiou HJ, Chou YH, Cheng SP, et al. Cubital tunnel syndrome: diagnosis by high-resolution ultrasonography. J Ultrasound Med 1998;17(10):643–648.
42. O'Driscoll SW, Horii E, Carmichael SW, Morrey BF. The cubital tunnel and ulnar neuropathy. J Bone Joint Surg Br 1991;73(4):613–617.
43. Okamoto M, Abe M, Shirai H, Ueda N. Morphology and dynamics of the ulnar nerve in the cubital tunnel: observation by ultrasonography. J Hand Surg [Br] 2000;25(1):85–89.
44. Husarik DB, Saupe N, Pfirrmann CWA, Jost B, Hodler J, Zanetti M. Elbow nerves: MR findings in 60 asymptomatic subjects—normal anatomy, variants, and pitfalls. Radiology 2009;252(1):148–156.
45. Reynolds DL Jr, Jacobson JA, Inampudi P, Jamadar DA, Ebrahim FS, Hayes CW. Sonographic characteristics of peripheral nerve sheath tumors. AJR Am J Roentgenol 2004;182(3):741–744.
46. Barr LL, Kirks DR. Ultrasonography of acute epitrochlear lymphadenitis. Pediatr Radiol 1993;23(1):72–73.
47. Craig JG, Jacobson JA, Moed BR. Ultrasound of fracture and bone healing. Radiol Clin North Am 1999;37(4):737–751, ix.
48. Takahara M, Shundo M, Kondo M, Suzuki K, Nambu T, Ogino T. Early detection of osteochondritis dissecans of the capitellum in young baseball players: report of three cases. J Bone Joint Surg Am 1998;80(6):892–897.
49. Dias JJ, Lamont AC, Jones JM. Ultrasonic diagnosis of neonatal separation of the distal humeral epiphysis. J Bone Joint Surg Br 1988;70(5):825–828.
50. Ziv N, Litwin A, Katz K, Merlob P, Grunebaum M. Definitive diagnosis of fracture-separation of the distal humeral epiphysis in neonates by ultrasonography. Pediatr Radiol 1996;26(7):493–496.

RadioGraphics

US of the Elbow: Indications, Technique, Normal Anatomy, and Pathologic Conditions

Gabrielle P. Konin, MD • Levon N. Nazarian, MD • Daniel M. Walz, MD

RadioGraphics 2013; 33:E125–E147 • **Published online** 10.1148/rg.334125059 • **Content Codes:** MK US

Page E131–E132
At the level of the proximal elbow, the radial nerve is located between the brachioradialis and brachialis muscles. At this level, it can be followed to its bifurcation into a superficial sensory branch and a deep motor branch. The superficial sensory branch courses in the forearm anterior to the brachioradialis muscle. The deep motor branch courses through the radial tunnel; as it exits, it pierces the superficial and deep portions of the supinator muscle as the PIN.

Page E133
The UCL is the chief stabilizer of the elbow against valgus stress when it is flexed more than 20°. The UCL consists of three bands (or bundles): anterior, posterior, and oblique. The anterior band or bundle can be divided into two bands, anterior and posterior, and is functionally the most important, as it provides the greatest degree of stabilization. The normal US appearance of the anterior band is a hyperechoic, thin, compact fibrillar band just deep to the common flexor tendon. It originates from the anteroinferior aspect of the medial epicondyle to insert on the sublime tubercle of the coronoid process of the ulna).

Page E135
Dynamic US of the ulnar nerve should be performed to evaluate for subluxation with or without snapping triceps syndrome. With the transducer in the transverse plane between the olecranon process and fixed at the medial epicondyle, the patient is asked to flex the elbow. This maneuver allows assessment of abnormal anterior and medial translation of the ulnar nerve over the medial epicondyle, with or without the medial head of the triceps muscle.

Page E136
Rupture of the DBT, best visualized in the longitudinal axis, appears as anechoic or hypoechoic discontinuity of tendon fibers with or without retraction and surrounding hypoechoic fluid). With a ruptured lacertus fibrosus, retraction of the tendon often occurs with nonvisualization of the distal tendon. The degree of tendon retraction does not necessarily indicate the status of the lacertus fibrosus, and US does not allow reliable visualization of a normal biceps aponeurosis or evidence of its rupture.

Page E137
The extensor carpi radialis brevis tendon of the common extensor tendon is universally involved, followed by the extensor digitorum communis and the remaining tendons and muscles of the extensor mechanism. In general, imaging is not indicated for evaluation of lateral epicondylitis but may be performed in complex, confounding, or recalcitrant cases. US is useful in assessing the severity and extent of tendon abnormality with the advantage of potential guided intervention.